A Target-Based Whole Cell Screen Approach To Identify Potential Inhibitors of *Mycobacterium tuberculosis* Signal Peptidase

Shilah A. Bonnett, Juliane Ollinger, Susantha Chandrasekera, Stephanie Florio, Theresa O'Malley, Megan Files, Jo-Ann Jee, James Ahn, Allen Casey, Yulia Ovechkina, David Roberts, Aaron Korkegian, and Tanya Parish*

TB Discovery Research, Infectious Disease Research Institute, 1616 Eastlake Avenue East, Suite 400, Seattle, Washington 98102, United States

S *Supporting Information*

ABSTRACT: The general secretion (Sec) pathway is a conserved essential pathway in bacteria and is the primary route of protein export across the cytoplasmic membrane. During protein export, the signal peptidase LepB catalyzes the cleavage of the signal peptide and subsequent release of mature proteins into the extracellular space. We developed a target-based whole cell assay to screen for potential inhibitors of LepB, the sole signal peptidase in *Mycobacterium tuberculosis*, using a strain engineered to underexpress LepB (LepB-UE). We screened 72,000 compounds against both the Lep-UE and wild-type (wt) strains. We identified the phenylhydrazone (PHY) series as having higher activity against the LepB-UE strain. We conducted a limited structure–activity relationship determination around a representative PHY compound with differential activity (MICs of 3.0 μM against the LepB-UE strain and 18 μM against the wt); several analogues were less potent against the LepB overexpressing strain. A number of chemical modifications around the hydrazone moiety resulted in improved potency. Inhibition of LepB activity was observed for a number of compounds in a biochemical assay using cell membrane fraction derived from *M. tuberculosis*. Compounds did not increase cell permeability, dissipate membrane potential, or inhibit an unrelated mycobacterial enzyme, suggesting a specific mode of action related to the LepB secretory mechanism.

KEYWORDS: *tuberculosis, signal peptidase, phenylhydrazones, phenotypic screen*
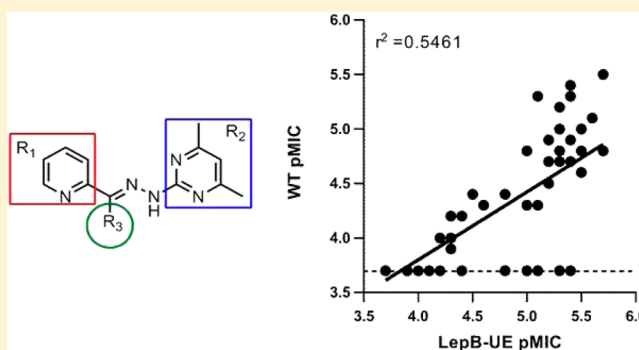
Mycobacterium tuberculosis, the causative agent of tuberculosis (TB), has plagued mankind for centuries and is one of the world's deadliest infectious diseases. In 2014, 9.6 million patients were diagnosed with TB infection and ~1.5 million people died.[1] Although the mortality rate has dropped by 47% since the 1990s, the emergence of multidrug resistant (MDR-TB) and extremely drug resistant (XDR-TB) strains has complicated our ability to control the disease. According to the World Health Organization (WHO), approximately 480,000 people developed MDR-TB in 2014 and the cure rate of those patients was only 50%.[1] Resistant strains are not susceptible to the standard drugs, and although MDR-TB is treatable using second-line drugs, such treatments are costly, toxic, and/or not readily available. Consequently, there is an urgent need for the development of new antitubercular therapies that are effective against resistant as well as persistent forms of tuberculosis. Ideally, new drugs should target essential pathways in *M. tuberculosis* that are not currently targeted by first- and second-line drugs.

The type I signal peptidase (SPase I), also known as the leader peptidase (LepB), is a key enzyme involved in protein secretion via the general secretion (Sec) pathway and is a potential drug target for tuberculosis.[2] Approximately 20% of all bacterial proteins synthesized are secreted, and they play vital roles in numerous processes, including nutrient uptake, pathogenicity, environmental response, resuscitation, cell wall biogenesis, and respiration.[3] The Sec pathway is highly conserved in bacteria and is the primary route involved in the export of proteins across the cytoplasmic membrane. LepB catalyzes the cleavage of the N-terminal signal peptide from preproteins during or shortly after translocation, releasing the mature protein into the extracellular space.[3] *M. tuberculosis* has a single LepB homologue, which is essential for cell viability.[2] Inhibiting LepB would prevent cleavage of the signal peptide from the preprotein; consequently, the proteins destined to be secreted would remain membrane bound.[4−8] Inhibition of LepB would also interfere with the translocation of proteins critical for various cellular processes and could ultimately lead to cell death.

Table 1. Strains and Plasmids Used in This Study

strain or plasmid	description	source or reference
plasmids		
pSM128	promoter probe vector-L5 integrase, *lacZ*, Sm	39
pINT7	pSM128 derivative lacking the *lacZ* gene	2
pCherry10	P_{G13}-mCherry in replicating vector, Hyg	42
pIKL-R1	P_{senX3} in pSM128	14
pTRP5	P_{trpE} in pSM128	15
pTRP7	P_{trpD} in pSM128	15
pLUSH5	$P_{gln\ E}$ in pSM128, Sm	16
pHIP1	$P_{Rv0251c}$ in pSM128, Sm	this study
pHIP2	$P_{Rv2466c}$ in pSM128, Sm	this study
pHIP3	$P_{Rv2745c}$ in pSM128, Sm	this study
pHIP4	P_{Rv2930} in pSM128, Sm	this study
pHIP5	P_{Rv0967} in pSM128, Sm	this study
pHIP6	P_{mbtI} in pSM128, Sm	this study
pUPPY1	P_{senX3}-*lepB* in integrating vector, L5 int, Sm	this study
pUPPY2	P_{trpE}-*lepB* in integrating vector, L5 int, Sm	this study
pUPPY3	P_{trpD}-*lepB* in integrating vector, L5 int, Sm	this study
pUPPY5	$P_{gln\ E}$-*lepB* in integrating vector, L5 int, Sm	this study
pUPPY6	$P_{Rv0251c}$-*lepB* in integrating vector, L5 int, Sm	this study
pUPPY7	$P_{Rv2466c}$-*lepB* in integrating vector, L5 int, Sm	this study
pUPPY8	$P_{Rv2745c}$-*lepB* in integrating vector, L5 int, Sm	this study
pUPPY9	P_{Rv2930}-*lepB* in integrating vector, L5 int, Sm	this study
pUPPY10	P_{Rv0967}-*lepB* in integrating vector, L5 int, Sm	this study
pUPPY11	P_{mbtI}-*lepB* in integrating vector, L5 int, Sm	this study
pUPPY13	native *lepB* in integrating vector, L5 int, Sm	this study
pOPPY4	P_{hsp60}-lepB in expression vector pSMT3, Hyg	14
M. tuberculosis strains		
H37Rv	wild-type	ATCC 25618
CHEAM3	H37Rv pluspCherry10 [P_{G13}-mCherry, Hyg]	19
SPAM13C	chromosomal *lepB* Δ; integrated [P_{lepB}-*lepB*, L5 int, Sm]; pCHERRY10 [mCherry, Hyg]	this study
SPAM15C	chromosomal *lepB* Δ; integrated [$P_{gln\ E}$-*lepB*, L5 int, Sm]; pCHERRY10 [mCherry, Hyg]	this study
SPAM17C	chromosomal *lepB* Δ; integrated [$P_{Rv2466c}$-LepB, L5 int, Sm]; pCHERRY10 [mCherry, Hyg]	this study
SPAM18C	chromosomal *lepB* Δ; integrated [$P_{Rv2745c}$-*lepB*, L5 int, Sm]; pCHERRY10 [mCherry, Hyg]	this study
SPAM19C	chromosomal *lepB* Δ; integrated [P_{Rv2930}-*lepB*, L5 int, Sm]; pCHERRY10 [mCherry, Hyg]	this study
SPAM20C	chromosomal *lepB* Δ; integrated [P_{senX3}-*lepB*, L5 int, Sm]; pCHERRY10 [mCherry, Hyg]	this study
SPAM22C	chromosomal *lepB* Δ; integrated [P_{trpE}-*lepB*, L5 int, Sm]; pCHERRY10 [mCherry, Hyg]	this study
SPAM23C	chromosomal *lepB* Δ; integrated [P_{trpD}-*lepB*, L5 int, Sm]; pCHERRY10 [mCherry, Hyg]	this study
LepB-OE	H37Rv; pOPPY4 [P_{hsp60}-*lepB*,pSMT3,Hyg]	this study

Bacterial SPases are membrane-bound endopeptidases belonging to the serine protease family S26[9] and are structurally and mechanistically distinct from their eukaryotic counterparts. Eukaryotic SPases utilize a catalytic triad composed for Ser-His-Asp residues, whereas bacterial SPases I use a unique Ser-Lys catalytic dyad mechanism.[10,11] In the proposed mechanism, the serine hydroxyl group from the bacterial SPase attacks the peptide substrate from the *si*-face rather than the *re*-face as seen in eukaryotic SPase.[11] Such differences can be exploited for the design of selective inhibitors of bacterial SPase I and should limit off-target toxicity. In addition to their unique catalytic mechanism and essentiality, another attractive feature of type I SPase as a potential drug target is the location of the catalytic domain on the extracellular surface, suggesting increased accessibility. Target-based whole cell screening strategies have been implemented in the identification of compounds targeting known biological targets within a cellular context.[12,13] Such strategies utilize conditional mutant strains exhibiting either reduced or enhanced expression levels of a particular target. One advantage of this strategy over a biochemical based approach is that it allows for the identification of active

inhibitors at a cellular level. Biochemical screening campaigns often lead to the identification of potent enzyme inhibitors, which lack whole cell activity due to poor penetration, rapid efflux, and/or inactivation. To examine the potential of LepB as an antitubercular target and to identify inhibitors potentially targeting protein secretion, we developed and implemented a target-based whole cell screen using a strain engineered with reduced expression of the sole, essential LepB homologue. Presented here are the results of our screen of 72,000 compounds against the wild-type (wt) and *lepB* under-expressing (LepB-UE) strains of *M. tuberculosis*. The screening campaign led to the identification of the phenylhydrazone series (PHY), which are more potent against the LepB-UE strain than the wt *M. tuberculosis*.

■ RESULTS AND DISCUSSION

We are interested in LepB, and more generally the secretory pathway and the secretome, as a drug target for novel antitubercular agents.[2] Therefore, we were interested in developing a target-based whole cell screen that could capture

both inhibitors acting on this mechanism while confirming potency against live bacteria.

Generation of the LepB underexpressing Strains. We first needed to construct a hypomorph, in which LepB expression was reduced as much as possible but still allowing for robust growth. We predicted this would give us strains that would be hypersusceptible to LepB inhibition, but would remain amenable to screening. To achieve this, we needed to construct stable strains in which LepB expression was reduced. Although we had previously generated strains in which LepB expression was under the control of a regulatable promoter (tetracycline-inducible system), these strains were not sufficiently stable for use in a high-throughput screen because they accumulated mutations that removed the inducibility of the promoter.[2] We generated a number of strains in which the only functional LepB allele was under the control of various *M. tuberculosis* promoters in order to find a suitable strain (Table 1).

We constructed recombinant strains by gene switching[17] and monitored both growth and the level of LepB mRNA. Expression of LepB from promoters $P_{Rv0251c}$, P_{Rv0967}, and P_{mbtl} did not result in viable strains. A reduction in LepB expression was seen with the remainder of the promoters tested, except P_{glnE} (Figure 1). Of note, expression from the native promoter
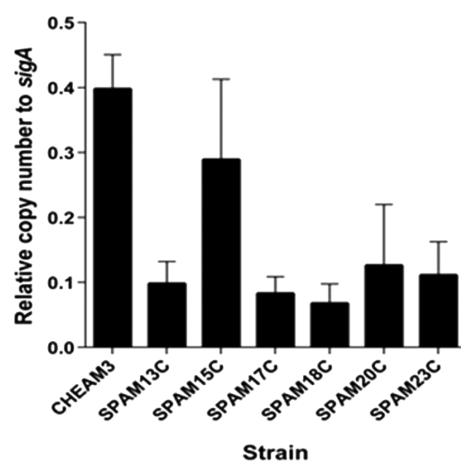

Figure 1. Expression levels of LepB. *M. tuberculosis* strains were grown in 7H9-Tw-OADC. mRNA levels were determined by RT-qPCR, and the results are normalized to *sigA* transcripts. Data are the mean ± standard deviation of three replicates. Strains of *M. tuberculosis* expressing codon-optimized mCherry were wild-type H37Rv (CHEAM3), and strains expressing LepB under the control of different promoters were SPAM13C-P_{lepB}, SPAM15C-$P_{gln E}$, SPAM17C-$P_{Rv2466c}$, SPAM18C-$P_{Rv2745c}$, SPAM20C-P_{senX3}, and SPAM23C-P_{trpD}.

at the L5 integration site was lower than in the wild-type strain; this phenomenon has been previously noted, in that general expression levels from promoters integrated at the L5 *att* site appear to be lower than in their native sites, possibly due to local effects such as supercoiling.[18]

We monitored growth of each strain in a tube and microplate format. Growth defects were seen with the underexpressing strains, which were more pronounced in 96-well plates when compared to wild-type. Small growth defects were seen in aerated liquid medium when grown in tubes except for SPAM19C, which showed a significant growth defect (Figure 2a). However, larger defects were seen in 384-well plates where

SPAM17C and SPAM18C showed a significant delay in growth (Figure 2b). Two strains (SPAM13C and SPAM15C) showed an intermediate growth phenotype with a slower growth rate than that of the wild-type. We measured the signal to background (S:B) for each strain. At day 5 all strains had S:B > 5, which is sufficient for screening. We selected SPAM13C for HTS assay development because it showed both lower levels of expression and a slight growth defect.

HTS Assay Development. We adapted our previous 96-well assay format for *M. tuberculosis* growth[19] to a 384-well format for single-point screening for both wild-type and SPAM13C (LepB-UE) strains. We varied a number of parameters to determine optimum assay conditions, which included bacterial cell density, length of assay, assay volume, and DMSO concentration. The assay was validated using standard robustness testing to determine interplate and interday variability according to NCGC guidelines.[20] The assay was run three times independently using conditions to produce minimum, midpoint, and maximum signals in duplicate. Statistical analysis was used to confirm that reproducibility met the appropriate criteria; Z' factor > 0.5 and % CV < 20% were attained, indicating a robust and reproducible assay (values were Z' 0.76−0.87; % CV 3.4−7.0). Maximum assay robustness and reproducibility were attained with the following assay conditions: 10 μL of bacterial culture at an OD_{590} = 0.06 and 20 μL of compound in 384-well plates incubated for 5 days at 37 °C. The final DMSO concentration was 2%, and the final compound concentration was 20 μM, respectively.

Primary Screen. We screened a library of ~72,000 diverse small molecules from our library (from ChemBridge) against both wt and the LepB-UE strains at 20 μM. Using a cutoff of 95% inhibition, the hit rate against the LepB-UE strain was 1.7% (1252 compounds), which was higher than the hit rate against the wt (1.3%, 949 compounds) (Figure 3). Of the 1252 compounds active against LepB-UE, 121 displayed greater activity as compared to the wt strain.

One hundred and eighty-nine compounds that inhibited growth ≥95% in either strain or that differentially inhibited the underexpressing LepB strain were selected for follow-up. Of this set, 21 compounds had a minimum inhibitory concentration (MIC) ≤ 20 μM against the LepB-UE strain and were also at least 2-fold more potent against the LepB-UE strain than the wt strain. Of these differential hits, 19 (**1−19**) belonged to the phenylhydrazone (PHY) class; compound **1** was the most potent (Table 2). Although there was only a single 1:1 comparator to compound **1**, the MICs revealed that different substitutions around the hydrazone moiety, including fused rings (**5−8**), acylhydrazones (**11−15**), picolinimidohydrazides (**16, 17**), hydrazinecarbothioamide (**18**), and hydrazinecarbodithioate (**19**), were tolerated.

Phenylhydrazone Structure−Activity Relationship (SAR). Hydrazones possess a wide range of pharmacological properties, including antimicrobial,[21−23] antitubercular,[24−31] anti-inflammatory,[32] and anticancer[33−35] activities. Hydrazone compounds that are derivatives of isoniazid or pyrazinamide have been reported with some activity against *M. tuber-culosis*.[24−31] The compounds we identified in our primary screen (**1−19**) and the analogues for the PHY series (**20−42**) had some structural similarity to isoniazid, but the pyrazole and picolinohydrazide derivatives (**43−56**) did not.

We selected the PHY series for further evaluation to see if we could improve potency and cytotoxicity. From our primary
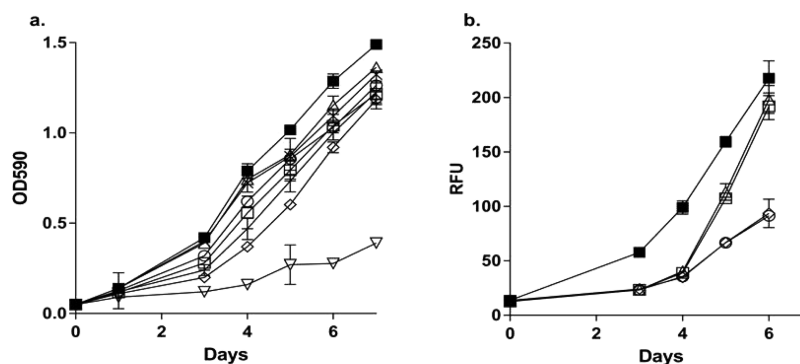
Figure 2. Growth of *M. tuberculosis* strains in aerobic culture. *M. tuberculosis* strains were grown in (a) growth tubes (data are the average ± standard deviation of three independent cultures) and (b) 384-well plates (data are the average ±standard deviation of all wells in the plate). Strains of *M. tuberculosis* expressing codon-optimized mCherry were wild-type H37Rv CHEAM3 (■), and strains expressing LepB under the control of different promoters were SPAM13C-P_{lepB} (△), SPAM15C-$P_{gln E}$ (□), SPAM17C-$P_{Rv2466c}$ (◇), SPAM18C-$P_{Rv2745c}$ (○), SPAM19C-P_{Rv2930} (▽), SPAM20C-P_{senX3} (×), and SPAM23C-P_{trpD} (+).
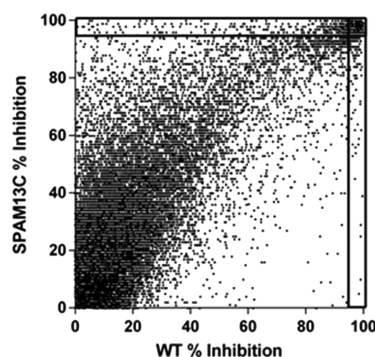

Figure 3. Primary screen. About 72,000 compounds were tested for inhibition of growth at a fixed concentration of 20 μM against wild-type and LepB-UE (SPAM13C) strains. Strains were grown in 384-well plates for 5 days in the presence of compound. Data are the percent growth inhibition compared to controls. A threshold for hits was set at 95% inhibition against either strain (highlighted in the bold boxes).

screen, compound **1** was the most active against the LepB-UE strain and was selected for limited SAR analysis to gain insight into the structural requirements for activity (Tables 3 and 4); 30 compounds were purchased commercially, and 8 compounds were synthesized and tested.

We first focused on activity against the LepB-UE strain (SPAM13C). Three segments of compound **1** (R₁, R₂, R₃) were examined (Table 3). Replacement of pyridine at R₁ with a furan (**20**), thiophene (**21**), phenyl (**22**), or phenol (**23, 24**) reduced the potency at least 10-fold (MIC = 30–90 μM), whereas activity was abolished with methyl (**25**) or pyridine (**26**) replacements. R₁ and R₃ substitutions with a phenyl group (**27**) had little impact on antitubercular activity compared to compound **1**.

Replacement of the 4,6-dimethylpyrimidine with a pyridine at R₂ (**29**) resulted in a 42-fold decrease in potency; however, activity was comparable to that of **1** when R₂ was substituted with either a triazinoindole (**28**), picolinimidohydrazide (**30**), or acylhydrazone (**31**) moiety. The potency of three additional picolinimidohydrazide (**32–34**) and six acylhydrazone derivatives (**35–40**) was examined. With the exception of **33**, the picolinimidohydrazide derivatives were moderately active (MIC = 41–106 μM). Two of the most potent compounds from the PHY series were acylhydrazone derivatives (**37** and **39**) with

MICs of 2–2.5 μM. Activity to comparable to that of **1** was observed when the R₂ group was replaced with a thioamide (**41**); however, a 16-fold decrease in activity was observed when it was replaced with a benzenesulfonyl group (**42**). Our data suggest that the R₁ position is rather sensitive to modifications and the pyridine group is the preferred functionality at R₁. The R₂ position tolerates a larger range of substitutions, and at the R₃ position, the methyl and phenyl groups were preferred. The data also suggest that the acylhydrazone moiety as seen in compounds **11–15, 31, 35, 37–40,** and **57** is well tolerated, with MIC values in the range of 3.5–15 μM.

To explore the impact of the hydrazone moiety upon activity, several substituted pyrazoles (**43–56**) and a picolinohydrazide (**57**) derivatives were tested (Table 4). Whereas the picolinohydrazide (**57**) exhibited activity similar to that of **1**, other pyrazole derivatives were detrimental to the antitubercular activity (MIC = 44–95 μM) or had no activity (MIC > 200 μM). We tested our compounds at a relatively high concentration (200 μM). Because our assay used a dual readout—both OD and RFU—we are able to identify solubility issues in the medium, normally seen as a discordance between the readouts. We did not see any issues with solubility in the microbiological medium that interfered with the measurement of growth used to determine MICs for the compounds tested.

Differential Activity. We were interested in finding compounds that targeted the secretory machinery and were potent against the wt strain. To determine if our series was truly active in this mechanism, we determined the activity against the wt strain and compared this to the LepB-UE strain. Differential activity, defined as >2-fold difference in MIC, was observed for 36 of 57 compounds (Figure 4a; Tables 2–4). In many cases the differences were small and the MICs were repeated multiple times to confirm the difference. For MICs where the difference was <10-fold, they were repeated a minimum of four times; for MICs with a differential of >10-fold, they were repeated twice. The differential we observed was consistent with an effect on LepB, because our expression levels were reduced by approximately 4-fold, such that we would not expect to see larger shifts in MIC.

Compounds **5, 8, 10, 14, 15, 17,** and **28** exhibited a differential >10, with compound **8** being 56-fold more potent toward the LepB-UE strain, and in fact all were inactive against the wt strain (MICs > 200 μM). The hydrazinecarbothioamide

Table 2. Biological Profile of PHY Compounds Identified from the Primary Screen

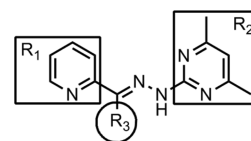| Cmpd #	Structure	LepB-UE MIC (μM)[a]	WT-MIC (μM)[c]	Cytotoxicity CC$_{50}$ (μM)[d]	LepB IC50 (μM)[e]
1		3.0 ± 1.1	18 ± 1	2.3	39
2		9.3 ± 3.2	43 ± 26	13	> 200
3		4.7[b]	11[b]	2.9	12
4		4.5 ± 2.5	10 ± 7	9.2	> 200
5		7.4 ± 3.4	> 200	5.0	> 200
6		3.8 ± 1.3	26 ± 12	8.7	> 200
7		3.9 ± 1.7	14 ± 3	5.2	130
8		3.6 ± 1.1	> 200	6.7	> 200
9		11 ± 1.0	57 ± 24	13	> 200
10		5.4 ± 2.6	> 200	4.3	> 200
11		3.5 ± 1.8	14 ± 7	6.1	26
12		6.3 ± 3.5	22 ± 2	34	> 200
13		4.7 ± 0.6	18 ± 5	21	> 200
14		4.9 ± 1.9	> 200	32	> 200
15		15 ± 2.5	> 200	63	> 200
16		10 ± 3.4	> 200	> 100	119
17		6.7 ± 1.6	48 ± 3	> 100	ND
18		9.0 ± 5.8	18 ± 12	11	ND
19		6.0 ± 4.2	10 ± 3	2.4	ND

[a]LepB-UE MIC values are minimum inhibitory concentrations (MIC) for *M. tuberculosis* strain SPAM13C. MICs are the average ± standard deviation of at least of two independent experiments unless otherwise noted. [b]Single MIC values were obtained. [c]Wild-type (wt) MIC are for *M. tuberculosis* strain. MICs are the average ± standard deviation of at least of two independent experiments unless otherwise noted. [d]CC$_{50}$ is the concentration required to inhibit Vero cells by 50%. [e]Not determined.

Table 3. Biological Profile of Analogues of Compound 1

Compound #	R$_1$	R$_2$	R$_3$	LepB-UE MIC (μM)[a]	WT MIC (μM)[c]	Cytotoxicity CC$_{50}$ (μM)[d]	LepB IC50 (μM)[e]
20			CH$_3$	82 ± 6	> 200	> 100	74
21			CH$_3$	94 ± 1	> 200	> 100	120
22			CH$_3$	67 ± 1	> 200	> 100	> 200
23			CH$_3$	54 ± 2	115[b]	> 100	140
24			CH$_3$	30 ± 3	40 ± 8	67	ND
25	CH$_3$		CH$_3$	> 200	> 200	> 100	ND
26			CH$_3$	> 200	> 200	ND	ND
27				2.2 ± 0.7	17 ± 8	0.1	> 200
28			CH$_3$	4.8 ± 2.4	> 200	1.2	87
29			CH$_3$	130[b]	> 200	> 100	ND
30			CH$_3$	7.7 ± 0.2	47 ± 6	59	ND
31			CH$_3$	3.6 ± 0.7	4.7 ± 0.3	10	ND
32			H	41[b]	59[b]	62	ND
33			H	> 200	> 200	> 100	ND
34			H	106[b]	> 200	> 100	ND
35			CH$_3$	8.2[b]	5.3 ± 3.3	0.6	ND
36			CH$_3$	26 ± 1	53 ± 2	12	> 200
37			CH$_3$	2.0 ± 0.5	4.2 ± 2.6	5.4	ND
38			CH$_3$	4.9 ± 0.2	17 ± 5	9.5	180
39			CH$_3$	2.5 ± 0.2	5.5 ± 1.4	3.3	> 200
40			CH$_3$	15 ± 1	42 ± 15	75	> 200
41			CH$_3$	3.6[b]	4.0[b]	22	ND
42			CH$_3$	48[b]	94[b]	> 100	34

[a]LepB-UE MIC values are minimum inhibitory concentrations (MIC) for *M. tuberculosis* strain SPAM13C. MICs are the average ± standard deviation of at least of two independent experiments unless otherwise noted. [b]Single MIC values were obtained. [c]Wild-type (wt) MICs are for *M. tuberculosis* strain. MICs are the average ± standard deviation of at least of two independent experiments unless otherwise noted. [d]CC$_{50}$ is the concentration required to inhibit Vero cells by 50%. [e]Not determined.

derivative (**41**), on the other hand, was equally potent toward both wt and LepB-UE.

Compounds **11** and **39** exhibited differential activity, but were also active against the wt strain with an MIC < 10 μM. Larger sets of analogues based on compounds **11** and **39** are needed to gain insight into the tolerability of the R$_2$ position.

LepB Activity Assay. The increased sensitivity of the LepB-UE strain to the PHY series could be due to a direct inhibitory effect on LepB, an effect on other components of the secretory pathway, or inhibition of a secreted protein. We wanted to determine if the series directly inhibits LepB. Purified active LepB is not available. We made substantial attempts to produce active protein in multiple expression systems, but were

unable to produce active folded protein (data not shown). LepB is an integral membrane protein, and its activity may be dependent on its correct folding within the membrane; therefore, we used purified membrane fractions to develop an in vitro assay for signal peptide cleavage. We used an internally quenched synthetic peptide substrate as the probe; cleavage of the peptide leads to fluorescence.[36] This assay has been used extensively to characterize the activity of various SPases from *Escherichia coli*, *Staphylococcus aureus*, and *Staphylococcus epidermidis*.[36−38]

We monitored peptide cleavage in the presence of selected compounds. MD3, a known inhibitor of LepB (Supporting Information Figure S1), was used as a control. In this assay MD3 has an IC$_{50}$ of 12 μM. Of the 57 compounds tested, 32

Table 4. Biological Profile for Pyrazole and Picolinohydrazide Derivatives

Cmpd #	Structure	LepB-UE MIC (μM)[a]	WT MIC (μM)[c]	Cytotoxicity CC$_{50}$ (μM)[d]	LepB IC$_{50}$ (μM)[e]
43		48 ± 2	115 ± 23	> 100	> 200
44		95 ± 7	> 200	> 100	> 200
45		56 ± 3	68 ± 12	> 100	ND
46		90 ± 28	> 200	> 100	> 200
47		61 ± 7	> 200	> 100	> 200
48		44 ± 6	> 200	> 100	ND
49		> 200	> 200	ND	ND
50		> 200	> 200	66	ND
51		> 200	> 200	> 100	ND
52		> 200	> 200	> 100	ND
53		> 200	> 200	> 100	ND
54		> 200	> 200	> 100	ND
55		> 200	> 200	> 100	ND
56		> 200	> 200	> 100	ND
57		3.9 ± 1.3	25 ± 4	32	64

[a]LepB-UE MIC values are minimum inhibitory concentrations (MIC) for *M. tuberculosis* strain SPAM13C. MICs are the average ± standard deviation of at least of two independent experiments unless otherwise noted. [b]Single MIC values were obtained. [c]Wild-type (wt) MICs are for *M. tuberculosis* strain. MICs are the average ± standard deviation of at least of two independent experiments unless otherwise noted. [d]CC$_{50}$ is the concentration required to inhibit Vero cells by 50%. [e]Not determined.

inhibited LepB activity by ≥40% at 200 μM (data not shown). We determined the IC$_{50}$ for each active compound (Figure 4b;

Tables 2−4). Of the 36 differentially active compounds, 10 had an IC$_{50}$ < 150 μM in the biochemical assay, with compound **3** being the most active with an IC$_{50}$ of 12 μM.

We did not see a correlation between the whole cell assay and the membrane assay (Figure 4). Our secretion assay was based on membrane fractions that could have other membrane proteins, lipids, and phospholipids present in higher relative amounts than in the whole cells, which could account for a lack of activity in this assay. Additionally, compounds that lack activity at the biochemical level could target other components of the secretory pathway or a secreted protein. We tested our compounds for activity against the unrelated protein IspC (Dxr), which catalyzes the second step in the non-mevalonate pathway of isoprenoid biosynthesis. IspC has a metal-dependent activity and has 10% sequence identity to LepB. No inhibition of IspC was seen (data not shown), suggesting that the compounds are not acting via nonspecific mechanisms.

Activity against Overexpressing Strain. We tested several compounds for activity against a LepB overexpressing strain. If compounds target LepB, we would expect that the overexpressing strain would be more resistant. We would be less likely to see this shift if compounds were targeting a secreted protein downstream, because overexpression of LepB would not affect the amount of the target protein produced. Eight differentially active compounds along with MD3 were tested against the LepB overexpressing strain (LepB-OE) (Table 5). MD3 has MICs of 7.5 and 27 μM against the LepB-UE and wt, respectively. When tested against the LepB-OE, an MIC of 35 μM was attained.

In particular compounds **2**, **27**, and **30** showed a clear pattern of decreased activity as LepB expression levels increased from the LepB-UE to the wt to the LepB-OE strain. All compounds showed a difference between at least two strains. This adds weight to our hypothesis that the compounds are targeting LepB directly. The lack of a linear relationship between MIC in the three strains could result from a number of reasons, because MICs measure the outcome of a number of parameters, which include compound penetration to the target, binding efficiency, off-rate of binding, and efflux. Measurements are complicated by the fact that inhibition of LepB itself is likely to affect permeability and cell wall composition, and this could directly affect compound efficacy. However, the trends seen across the series increase our confidence that there is a bona fide inhibition.
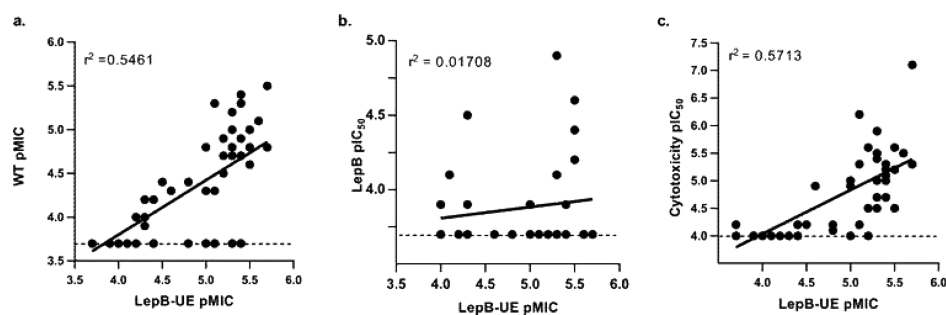

Figure 4. Correlation between potency, cytotoxicity, and biochemical activity. Plots of (a) pMIC LepB-UE versus pMIC wt for 58 PHY compounds and (b) pMIC LepB-UE versus pIC50 purified membrane fractions for 32 PHY compounds. Compounds were selected for evaluation in the biochemical assay according to the established criteria (%I > 40). (c) Plot of pMIC LepB-UE versus pIC$_{50}$ Vero cells for 58 compounds. The limit of detection, as indicated by the dashed line, is 200 μM for both the cellular and biochemical assays and 100 μM for the cytotoxicty assay involving Vero cells.

Table 5. Comparison of MICs against Different Strains

compound	LepB-UE MIC^a (μM)	WT MIC^b (μM)	LepB-OE MIC^c (μM)
1	3.0 ± 1.1	18 ± 1	18 ± 8
2	9.3 ± 3.2	43 ± 26	160 ± 57
11	3.5 ± 1.8	14 ± 7	5.6 ± 0.6
27	2.2 ± 0.7	17 ± 8	103 ± 38
30	7.7 ± 0.2	47 ± 6	>200
38	4.9 ± 0.2	17 ± 5	9.2 ± 4.0
39	2.5 ± 0.2	5.5 ± 1.4	6.5 ± 2.2
40	15 ± 1	42 ± 15	27 ± 2

^{a}LepB-UE MIC values are minimum inhibitory concentrations (MIC) for *M. tuberculosis* strain SPAM13C. MICs are the average ± standard deviation of at least of two independent experiments unless otherwise noted. ^{b}Wild-type (wt) MICs are for *M. tuberculosis* strain. MICs are the average ± standard deviation of at least of two independent experiments unless otherwise noted. ^{c}LepB-OE MICs are for *M. tuberculosis* strain expressing LepB under the hsp60 promotor. MICs are the average ± standard deviation of at least of two independent experiments unless otherwise noted.

Membrane Permeability Assay. To determine whether compound treatment increased membrane permeability, we examined the accumulation of ethidium bromide (Figure 5).
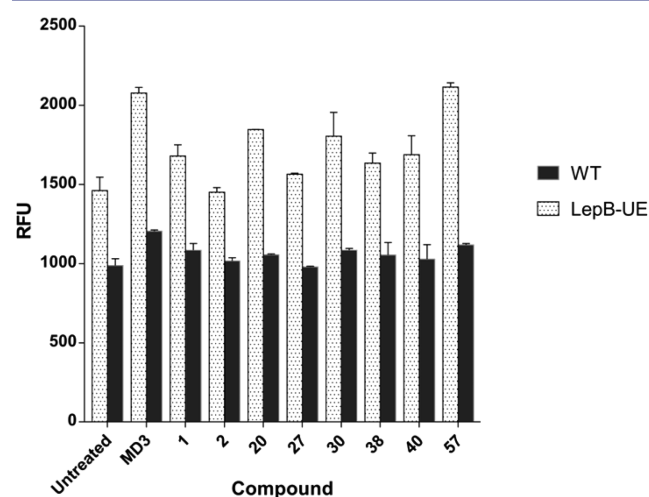

Figure 5. Permeability of *M. tuberculosis* strains. Permeability was assessed by monitoring uptake of ethidium bromide. Strains were exposed to compounds, MD3 (control), or untreated. Each assay was carried out twice. Data are the mean ± SD.

Interestingly, LepB-UE was slightly more permeable as compared to the wild-type, suggesting some alterations in cell wall structure. The small increase in permeability did not significantly affect sensitivity to rifampicin: MICs of 7.7 ± 2.3 nM against wt and 5.4 ± 0.9 nM against LepB-UE. However, treatment with PHY analogues did not change permeability, either in the wild-type or in the LepB-UE strain. Thus, the compounds had no direct effect on permeabilizing bacterial cells. We also looked at the effect of compounds on membrane potential, but none of the compounds had any effect (Supporting Information Figure S2).

Selectivity. We looked at the selectivity of the PHY series for bacterial cells. Most compounds had some level of cytotoxicity against Vero cells with low selectivity index (SI < 3) (Figure 4c; Tables 2−4). One compound (16), a picolinimidohydrazide derivative, had SI > 10, suggesting

potential for improvement. The activity of additional picolinimdioylhydrazide derivatives was evaluated. Substituting the R$_1$ hydroxyl group of 16 with either a hydrogen (34) or a methoxy (33) group resulted in a 15-fold decrease in selectivity. The observed decrease in selectivity for these compounds was the result of a decrease in potency against the LepB-UE concomitant with a loss of activity against the wt strain. Whereas the removal of the R$_1$ nitro group from 16, as seen with compound 17, had little impact upon potency against LepB-UE and cytotoxicity, a ~4-fold increase in potency against wt was observed. Differentially active compound 57 also had SI > 10 and was active against wt (MIC = 25 μM). We need additional SAR evaluation to understand how chemical modification around the hydrazone moiety directly influences the potency and selectivity.

■ CONCLUSION

We developed and implemented a high-throughput screen using an *M. tuberculosis* strain engineered with reduced LepB expression to allow the identification of weak inhibitors of *M. tuberculosis* growth. We identified the PHY series that was more potent against the LepB-UE strain than against the wt strain. We conducted a focused SAR study and determined that we were able to generate compounds with activity against the wt strain, which also retained the differential activity. Thus, our strategy of starting with "weak" inhibitors selected by the LepB-UE was validated. The PHY series had differential activity against recombinant LepB strains and demonstrated inhibition of LepB in a membrane fraction assay. Furthermore, we did not observe an increase in ethidium bromide accumulation for wt or Lep-UE strains upon treatment with a select number of PHY compounds. Taken together, this suggests the possibility that the series targets LepB directly, rather than a downstream secreted protein or by increased permeability due to cell wall alteration. Cytotoxicity was a problem with this series, although we identified one compound with good selectivity, suggesting a path forward. Future work to progress the PHY series into lead compounds would address cytotoxicity/selectivity as well as confirm the mode of action on LepB.

■ METHODS

Bacterial Culture. The *M. tuberculosis* strains and plasmids used in this study are summarized in Table 1. All strains were maintained in Middlebrook 7H9 medium supplemented with 0.5% w/v Tween 80 and 10% v/v oleic acid albumin dextrose catalase (OADC) supplement (7H9-Tw-OADC) or on Middlebrook 7H10 agar plus 10% v/v OADC. Hygromycin B was added to 50 μg/mL when necessary.

Construction of Recombinant *M. tuberculosis* Strains. Several expression plasmids were constructed in which LepB was placed under the control of different promoters. A native expression construct with *LepB* under the control of its native promoter (pUPPY13) was made by PCR amplification using primer pair P1lepB-F1 5′ <u>CGA ATT C</u>CT GTA CTA CCT GCG CGA A 3′ and PlepB-R 5′ <u>CAG GGC GCC ACT ACT A</u>AT GGC TAC CGA CCT TGC T 3′ and subcloning into pINT7 as *Eco*RI and *Kas*I fragments. The LepB gene was amplified using primer pair NPlepB_F1 5′ AAG CTT GTG ACC GAA ACC ACG GAC TC 3′ and NPlepB_R3 5′ CGT CGA CTA CTA ATG GCT ACC GAC CTT GC 3′ and cloned into promoter-expression constructs containing P$_{senX}$, P$_{trpECBA}$, P$_{trpD}$, P$_{glnE}$, P$_{Rv0251c}$, P$_{Rv2466c}$, P$_{Rv2745c}$, P$_{Rv2930}$, P$_{Rv0967}$, or

P$_{mbtl}$ in an integrating plasmid based on pSM128 (containing the L5 integrase, attP site, and SmR) by replacing the LacZ with LepB (HindIII−SalI fragment).[39]

M. tuberculosis strains were constructed by gene switching.[17] A strain of *M. tuberculosis* in which a functional LepB (under the control of a tetracycline-inducible promoter) was provided on an integrating plasmid (HygR) and the normal chromosomal copy was deleted (in-frame, unmarked deletion) was used.[2] Expression plasmids carrying LepB under the control of various heterologous promoters together with the L5 integrase/attP site and streptomycin resistance gene (SmR) were constructed. Each plasmid was switched into the del-int strain by electroporation and selection on streptomycin; replacement of the resident plasmid was confirmed by testing for hygromycin sensitivity.

A LepB overexpressing strain (LepB-OE) was constructed by electroporating pOPPY4, an expression plasmid in which *lepB* was under the control of the hsp60 promoter,[2] into *M. tuberculosis* H37Rv.

Measurement of LepB mRNA Transcripts. Total *M. tuberculosis* RNA was extracted as previously described.[40] A two-step quantitative reverse transcriptase PCR using the TaqMan Gene Expression Master Mix (ThermoFisher Scientific) was performed according to the manufacturer's instructions using *lepB* and *sigA* specific primer−probe sets: *lepB*-TaqManF1 (5′-GGT GCT GGC GGT GAT TG-3′), *lepB*-TaqManR1 (5′-AAG GGC GCG CGA CAA-3′), and *lepB*-MGB probe (5′-AAG GGC GCG CGA CAA-3′); *sigA*-TaqMan F1 (5′-CCG ATG ACG ACG AGG AGA TC-3′), *sigA*-TaqMan R1 (5′-GGC CTC CGA CTC GTC TTC A-3′), and *sigA*-MGB probe (5′-CCT CCG GTG ATT TC-3′). Transcript copy numbers were calculated using standard curves for each gene generated with genomic DNA. Controls including no RT reaction were used to control for DNA contamination. The transcript level of *lepB* was normalized to the transcript levels of *sigA*, a housekeeping sigma factor.[41]

HTS and MIC Determination. A chemically diverse small molecule library from ChemBridge was screened against the wt and LepB-UE strains. Compounds were diluted to 1 mM in DMSO and screened at a final concentration of 20 μM. Fluorescent strains of *M. tuberculosis* expressing codon-optimized mCherry were generated by electroporating pCherry10[42] into wt and recombinant strains. Strains were grown in 7H9-OADC-Tw to an OD$_{590}$ of 0.8−0.9 and diluted to a theoretical OD$_{590}$ of 0.06. The assay conditions for screening were as follows: 10 μL of culture was dispensed into black, clear-bottomed 384-well microplates containing 20 μL of 7H9-Tw-OADC-DMSO containing test compound (final DMSO and compound concentrations of 2% and 20 μM, respectively). Plates were incubated for 5 days at 37 °C in high humidity, and growth was monitored by OD$_{590}$ and/or fluorescence (Ex 589 nm/Em 614 nm).[19] Each assay plate included controls in columns 1, 2, 23, and 24 as follows: columna 1 and 23, maximum inhibition (2 μM rifampicin); column 2, minimum inhibition (2% DMSO); column 24, contamination control (no inoculum). Results were analyzed and managed using the Web-based software from the Collaborative Drug Discovery (CDD). The % CV and Z′ values for each assay plate were calculated.

MICs were determined against wt, LepB-UE, and LepB overexpressing (LepB-OE) strains according to published methods.[19] A 10-point 2-fold serial dilution was carried out on each of compounds from a starting concentration of 10 mM

such that the final assay concentration ranged from 200 μM to 10 nM. Bacterial growth was measured by OD$_{590}$ after 5 days of incubation at 37 °C in 96-well, black, clear-bottomed plates. Results were analyzed and managed using the Web-based software from the Collaborative Drug Discovery (CDD). A nonlinear least-squares curve was generated to calculate the MICs. The dose−response experiment was carried out at least four times for those compounds with a differential activity between 2 and 10 and at least two times for those with a differential activity >10.

LepB Membrane Assay. Cell membrane fractions were isolated from γ-irradiated whole *M. tuberculosis* H37Rv (NR-14819; BEI resources). Cells (10 g) were washed once in 100 mL of 20 mM Tris (pH 8.0), 250 mM NaCl, and 0.05% w/v Tween 80 buffer and suspended in 80 mL of 20 mM Tris, pH 8, and 1% Triton X-114. The suspension was incubated for 1 h with rotation, and the pellet was recovered by centrifugation. One hundred milligrams of Triton X-114 membrane fraction pellet was solubilized in 1 mL of XTractor buffer (Clontech) and transferred to a 2 mL screw-cap tube containing 0.1 mm silica. The tubes were agitated in a BeadBeater (BioSpec) for five 30 s pulses. The resulting cell membrane fraction was diluted 1:5 with 50 mM Tris-HCl, pH 8.0, and assayed for SPase activity using the fluorogenic peptide substrate 3-nitrotyrosine (NO)-YFSASALA∼KI-aminobenzoic acid-OH (ABZ) (California Peptide). Assays were performed in 96-well black plates with 2 μM substrate, 200 μM test compound, and 3% DMSO in 50 mM Tris-HCl, pH 8.0 (total volume = 100 μL). Reactions were initiated by the addition of 10 μL of cell membrane fraction and incubated at 37 °C for 4 h. Activity was analyzed by fluorescence (Ex 315 nm/Em 410 nm). Each assay plate contained controls with no compound or no cell membrane fraction. Dose−response was carried out for all compounds exhibiting an inhibition of ≥40%.

Membrane Permeability. Cell permeability was assessed by monitoring uptake of ethidium bromide.[43] Strains were grown to an OD$_{590}$ of 0.8−0.9, harvested, washed three times in PBS and 0.05% w/v Tween 80, and resuspended in PBS and 0.05% w/v Tween 80 buffer to a final OD$_{590}$ of 0.8. Aliquots (50 μL) were dispensed into black, clear-bottomed, 96-well microplates containing 50 μL of PBS, 0.05% w/v Tween 80, 8 μg/mL ethidium bromide, and test compound (final DMSO and compound concentrations of 2% and 200 μM, respectively). The accumulation of EtBr was determined by monitoring the increase in fluorescence (Ex 530 nm/Em 590 nm) over a 90 min period while the plates were incubated at 37 °C.

Membrane Potential. Membrane potential was determined using the cationic dye DiOC$_2$. Cells were grown to an OD$_{590}$ of 0.8−0.9, harvested, and washed three times in 7H9 lacking OADC. Bacteria were resuspended in 7H9 (no OADC) to an OD$_{590}$ of 1, incubated with DiOC$_2$ for 20 min at room temperature, and harvested. Bacteria were resuspended in the same volume of 7H9 (no OADC) and aliquoted (50 μL) into black, clear-bottomed, 96-well microplates containing 50 μL of medium and test compound (final DMSO and compound concentrations of 2% and 200 μM, respectively). Cells were incubated at room temperature for 45 min, fluorescence was measured at Ex 488 nm/Em 530 nm and Ex 488 nm/Em 610 nm, and the ratio was calculated.

Cytotoxicity. Cytotoxicity against African green monkey adult kidney cell (Vero cells) was determined as previously described using CellTiter-Glo reagent.[44] The concentration

causing 50% growth inhibition (IC_{50}) was calculated by fitting the inhibition curves using the Levenberg−Marquardt algorithm.

Chemical Synthesis. The synthesis of phenylhydrazones (PHY) was achieved by dissolving 1 equiv of the acid with 1 equiv of the hydrazine in anhydrous ethanol. After refluxing the reaction overnight, the acetone was evaporated off, and the crude reaction mixture was purified by column chromatography. ^{1}H and NMR spectral data were recorded in $CDCl_3$ or acetone-d_6 on a 300 MHz Bruker NMR spectrometer. Column chromatography was conducted on Revelaris flash chromatography system. Reactions were monitored using thin-layer chromatography (TLC) on silica gel plates. HPLC analysis was conducted on an Agilent 1100 series LC system (Agilent ChemStation Rev.A.10.02; Phenomenex-Luna-C18, 4.8 mm × 150 mm, 5 μm, 1.0 mL/min, UV 254 nm, room temperature) with MeCN/H_2O (0.05% TFA or HCOOH buffer) gradient elution. HPLC-MS was performed on a Gilson 321 HPLC with detection performed by a Gilson 170 DAD and a Finnigan AQA mass spectrometer operating in electrospray ionization mode using a Phenomenex Gemini C18 150 × 4.6 mm column. Unless noted, all chemicals were purchased pure, from commercially available sources such as Sigma-Aldrich, Enamine, Chembridge, Fisher, or other chemical vendors. All reagents and solvents were used as received. Compounds **25**, **27**, **29**, **33**, **34**, **42**, and **58** are known compounds that can be purchased commercially. Compounds **30**,[45−47] **32**,[48] and **42**[49,50] were prepared according to modified literature procedures.

■ ASSOCIATED CONTENT

Ⓢ Supporting Information

The Supporting Information is available free of charge on the ACS Publications website at DOI: 10.1021/acsinfecdis.6b00075.

> Figure S1, structure and activity of MD3; Figure S2, impact of compounds on membrane potential (PDF)

■ AUTHOR INFORMATION

Corresponding Author

*(T.P.) E-mail: tanya.parish@idri.org.

Notes

The authors declare no competing financial interest.

■ ACKNOWLEDGMENTS

■ REFERENCES

(1) WHO. (2015) *Global Tuberculosis Report*, Geneva, Switzerland.

(2) Ollinger, J., O'Malley, T., Ahn, J., Odingo, J., and Parish, T. (2012) Inhibition of the sole type I signal peptidase of *Mycobacterium tuberculosis* is bactericidal under replicating and nonreplicating conditions. *J. Bacteriol.* 194, 2614−2619.

(3) Feltcher, M. E., Sullivan, J. T., and Braunstein, M. (2010) Protein export systems of *Mycobacterium tuberculosis*: novel targets for drug development? *Future Microbiol.* 5, 1581−1597.

(4) Dalbey, R. E., and Wickner, W. (1985) Leader peptidase catalyzes the release of exported proteins from the outer surface of the *Escherichia coli* plasma membrane. *J. Biol. Chem.* 260, 15925−15931.

(5) Koshland, D., and Botstein, D. (1982) Evidence for posttranslational translocation of β-lactamase across the bacterial inner membrane. *Cell* 30, 893−902.

(6) Koshland, D., Sauer, R. T., and Botstein, D. (1982) Diverse effects of mutations in the signal sequence on the secretion of β-lactamase in *Salmonella* typhimurium. *Cell* 30, 903−914.

(7) Kuhn, A., and Wickner, W. (1985) Conserved residues of the leader peptide are essential for cleavage by leader peptidase. *J. Biol. Chem.* 260, 15914−15918.

(8) Fikes, J. D., and Bassford, P. J. (1987) Export of unprocessed precursor maltose-binding protein to the periplasm of *Escherichia coli* cells. *J. Bacteriol.* 169, 2352−2359.

(9) Ekici, Ö. D., Paetzel, M., and Dalbey, R. E. (2008) Unconventional serine proteases: variations on the catalytic Ser/His/Asp triad configuration. *Protein Sci.* 17, 2023−2037.

(10) Black, M. T. (1993) Evidence that the catalytic activity of prokaryote leader peptidase depends upon the operation of a serine-lysine catalytic dyad. *J. Bacteriol.* 175, 4957−4961.

(11) Tschantz, W. R., Sung, M., Delgado-Partin, V. M., and Dalbey, R. E. (1993) A serine and a lysine residue implicated in the catalytic mechanism of the *Escherichia coli* leader peptidase. *J. Biol. Chem.* 268, 27349−27354.

(12) Abrahams, Garth, L., Kumar, A., Savvi, S., Hung, Alvin, W., Wen, S., Abell, C., Barry, C. E., III, Sherman, David, R., Boshoff, Helena, I. M., and Mizrahi, V. (2012) Pathway-Selective Sensitization of *Mycobacterium tuberculosis* for Target-Based Whole-Cell Screening. *Chem. Biol.* 19, 844−854.

(13) Kumar, A., Zhang, M., Zhu, L., Liao, R. P., Mutai, C., Hafsat, S., Sherman, D. R., and Wang, M.-W. (2012) High-throughput screening and sensitized bacteria identify an *M. tuberculosis* dihydrofolate reductase inhibitor with whole cell activity. *PLoS One* 7, e39961.

(14) Roberts, G., Vadrevu, I. S., Madiraju, M. V., and Parish, T. (2011) Control of CydB and GltA1 expression by the SenX3 RegX3 two component regulatory system of *Mycobacterium tuberculosis*. *PLoS One* 6, e21090.

(15) Parish, T. (2003) Starvation survival response of *Mycobacterium tuberculosis*. *J. Bacteriol.* 185, 6702−6706.

(16) Pashley, C. A., Brown, A. C., Robertson, D., and Parish, T. (2006) Identification of the *Mycobacterium tuberculosis* GlnE promoter and its response to nitrogen availability. *Microbiology* 152, 2727−2734.

(17) Pashley, C. A., Parish, T., McAdam, R. A., Duncan, K., and Stoker, N. G. (2003) Gene replacement in mycobacteria by using incompatible plasmids. *Appl. Environ. Microbiol.* 69, 517−523.

(18) Huff, J., Czyz, A., Landick, R., and Niederweis, M. (2010) Taking phage integration to the next level as a genetic tool for mycobacteria. *Gene* 468, 8−19.

(19) Ollinger, J., Bailey, M. A., Moraski, G. C., Casey, A., Florio, S., Alling, T., Miller, M. J., and Parish, T. (2013) A dual read-out assay to evaluate the potency of compounds active against *Mycobacterium tuberculosis*. *PLoS One* 8, e60531.

(20) NCGC. (2004) *Assay Guidance Manual*, Bethesda, MD.

(21) Khan, S. A., and Yusuf, M. (2009) Synthesis, spectral studies and in vitro antibacterial activity of steroidal thiosemicarbazone and their palladium (Pd(II)) complexes. *Eur. J. Med. Chem.* 44, 2270−2274.

(22) Loncle, C., Brunel, J. M., Vidal, N., Dherbomez, M., and Letourneux, Y. (2004) Synthesis and antifungal activity of cholesterol-hydrazone derivatives. *Eur. J. Med. Chem.* 39, 1067−1071.

(23) Vicini, P., Zani, F., Cozzini, P., and Doytchinova, I. (2002) Hydrazones of 1,2-benzisothiazole hydrazides: synthesis, antimicrobial activity and QSAR investigations. *Eur. J. Med. Chem.* 37, 553−564.

(24) Bedia, K.-K., Elçin, O., Seda, U., Fatma, K., Nathaly, S., Sevim, R., and Dimoglo, A. (2006) Synthesis and characterization of novel

hydrazide—hydrazones and the study of their structure—antituberculosis activity. *Eur. J. Med. Chem.* 41, 1253−1261.

(25) Küçükgüzel, Ş. G., Rollas, S., Küçükgüzel, I., and Kiraz, M. (1999) Synthesis and antimycobacterial activity of some coupling products from 4-aminobenzoic acid hydrazones. *Eur. J. Med. Chem.* 34, 1093−1100.

(26) Sriram, D., Yogeeswari, P., and Madhu, K. (2005) Synthesis and in vitro and in vivo antimycobacterial activity of isonicotinoyl hydrazones. *Bioorg. Med. Chem. Lett.* 15, 4502−4505.

(27) Ventura, C., and Martins, F. (2008) Application of Quantitative Structure—Activity Relationships to the Modeling of Antitubercular Compounds. 1. The Hydrazide Family. *J. Med. Chem.* 51, 612−624.

(28) Imramovský, A., Polanc, S., Vinšová, J., Kočevar, M., Jampílek, J., Rečková, Z., and Kaustová, J. (2007) A new modification of antitubercular active molecules. *Bioorg. Med. Chem.* 15, 2551−2559.

(29) Maccari, R., Ottanà, R., and Vigorita, M. G. (2005) In vitro advanced antimycobacterial screening of isoniazid-related hydrazones, hydrazides and cyanoboranes: Part 14. *Bioorg. Med. Chem. Lett.* 15, 2509−2513.

(30) Vavříková, E., Polanc, S., Kočevar, M., Košmrlj, J., Horváti, K., Bősze, S., Stolaříková, J., Imramovský, A., and Vinšová, J. (2011) New series of isoniazid hydrazones linked with electron-withdrawing substituents. *Eur. J. Med. Chem.* 46, 5902−5909.

(31) Vergara, F. M. F., Lima, C. H. d. S., Henriques, M. d. G. M. d. O., Candéa, A. L. P., Lourenço, M. C. S., Ferreira, M. d. L., Kaiser, C. R., and de Souza, M. V. N. (2009) Synthesis and antimycobacterial activity of *N′*-[(*E*)-(monosubstituted-benzylidene)]-2-pyrazinecarbohydrazide derivatives. *Eur. J. Med. Chem.* 44, 4954−4959.

(32) Todeschini, A. R., de Miranda, A. L. P., da Silva, K. C. M., Parrini, S. C., and Barreiro, E. J. (1998) Synthesis and evaluation of analgesic, antiinflammatory and antiplatelet properties of new 2-pyridylarylhydrazone derivatives. *Eur. J. Med. Chem.* 33, 189−199.

(33) Andreani, A., Burnelli, S., Granaiola, M., Leoni, A., Locatelli, A., Morigi, R., Rambaldi, M., Varoli, L., Calonghi, N., Cappadone, C., Farruggia, G., Zini, M., Stefanelli, C., Masotti, L., Radin, N. S., and Shoemaker, R. H. (2008) New antitumor imidazo[2,1-*b*]thiazole guanylhydrazones and analogues. *J. Med. Chem.* 51, 809−816.

(34) Hu, W.-x., Zhou, W., Xia, C.-n., and Wen, X. (2006) Synthesis and anticancer activity of thiosemicarbazones. *Bioorg. Med. Chem. Lett.* 16, 2213−2218.

(35) Vicini, P., Incerti, M., Doytchinova, I. A., La Colla, P., Busonera, B., and Loddo, R. (2006) Synthesis and antiproliferative activity of benzo[*d*]isothiazole hydrazones. *Eur. J. Med. Chem.* 41, 624−632.

(36) Zhong, W., and Benkovic, S. J. (1998) Development of an internally quenched fluorescent substrate for *Escherichia coli* leader peptidase. *Anal. Biochem.* 255, 66−73.

(37) Bockstael, K., Geukens, N., Rao, C. V. S., Herdewijn, P., Anné, J., and Van Aerschot, A. (2009) An easy and fast method for the evaluation of *Staphylococcus epidermidis* type I signal peptidase inhibitors. *J. Microbiol. Methods* 78, 231−237.

(38) Rao, S., Bockstael, K., Nath, S., Engelborghs, Y., Anné, J., and Geukens, N. (2009) Enzymatic investigation of the *Staphylococcus aureus* type i signal peptidase SpsB − implications for the search for novel antibiotics. *FEBS J.* 276, 3222−3234.

(39) Dussurget, O., Timm, J., Gomez, M., Gold, B., Yu, S., Sabol, S. Z., Holmes, R. K., Jacobs, W. R., and Smith, I. (1999) Transcriptional control of the iron-responsive *fxbA* gene by the mycobacterial regulator IdeR. *J. Bacteriol.* 181, 3402−3408.

(40) Rustad, T. R., Roberts, D. M., Liao, R. P., and Sherman, D. R. (2009) Isolation of mycobacterial RNA. In *Mycobacteria Protocols*, 2nd ed. (Parish, T., and Brown, C. A., Eds.), pp 13−22, Humana Press, Totowa, NJ, USA.

(41) Miller, J. H. (1972) Assay of *β*-galactosidase activity. In *Experiments in Molecular Genetics*, pp 352−355, Cold Spring Harbor Laboratory Press, Cold Spring Harbor, NY, USA.

(42) Carroll, P., Schreuder, L. J., Muwanguzi-Karugaba, J., Wiles, S., Robertson, B. D., Ripoll, J., Ward, T. H., Bancroft, G. J., Schaible, U. E., and Parish, T. (2010) Sensitive Detection of Gene Expression in Mycobacteria under Replicating and Non-Replicating Conditions Using Optimized Far-Red Reporters. *PLoS One* 5, e9823.

(43) Rodrigues, L., Viveiros, M., and Aínsa, J. A. (2015) Measuring Efflux and Permeability in Mycobacteria. In *Mycobacteria Protocols*, pp 227−239 (Parish, T., and Roberts, M. D., Eds.), Springer, New York.

(44) Chandrasekera, N. S., Alling, T., Bailey, M. A., Files, M., Early, J. V., Ollinger, J., Ovechkina, Y., Masquelin, T., Desai, P. V., Cramer, J. W., Hipskind, P. A., Odingo, J. O., and Parish, T. (2015) Identification of phenoxyalkylbenzimidazoles with antitubercular activity. *J. Med. Chem.* 58, 7273−7285.

(45) Gokhale, N. H., Padhye, S. S., Padhye, S. B., Anson, C. E., and Powell, A. K. (2001) Copper complexes of carboxamidrazone derivatives as anticancer agents. 3. Synthesis, characterization and crystal structure of [Cu(appc)Cl2], (appc = N1-(2-acetylpyridine)-pyridine-2-carboxamidrazone. *Inorg. Chim. Acta* 319, 90−94.

(46) Yue, Y.-F., Fang, C.-J., Gao, E.-Q., He, C., Bai, S.-Q., Xu, S., and Yan, C.-H. (2008) Four thiocyanato-bridged cadmium(II) polymeric complexes based on open chain diazine ligands. *J. Mol. Struct.* 875, 80−85.

(47) Yue, Y.-F., Gao, E.-Q., Fang, C.-J., Zheng, T., Liang, J., and Yan, C.-H. (2008) The crystal structures of four azido-bridged Zn(II) complexes based on open-chain diazine Schiff-base ligands. *CrystEngComm* 10, 614−622.

(48) Szocs, B., Bokor, E., Szabo, K. E., Kiss-Szikszai, A., Toth, M., and Somsak, L. (2015) Synthesis of 5-aryl-3-*C*-glycosyl- and unsymmetrical 3,5-diaryl-1,2,4-triazoles from alkylidene-amidrazones. *RSC Adv.* 5, 43620−43629.

(49) De Monte, C., Carradori, S., Secci, D., D'Ascenzio, M., Guglielmi, P., Mollica, A., Morrone, S., Scarpa, S., Aglianò, A. M., Giantulli, S., and Silvestri, I. (2015) Synthesis and pharmacological screening of a large library of 1,3,4-thiadiazolines as innovative therapeutic tools for the treatment of prostate cancer and melanoma. *Eur. J. Med. Chem.* 105, 245−262.

(50) D'Ascenzio, M., Chimenti, P., Gidaro, M. C., De Monte, C., De Vita, D., Granese, A., Scipione, L., Di Santo, R., Costa, G., Alcaro, S., Yáñez, M., and Carradori, S. (2015) (Thiazol-2-yl)hydrazone derivatives from acetylpyridines as dual inhibitors of MAO and AChE: synthesis, biological evaluation and molecular modeling studies. *J. Enzyme Inhib. Med. Chem.* 30, 908−919.